Proceedings of the IASTED International Conference
APPLIED SIMULATION AND MODELLING
September 3-5, 2003, Marbella, Spain

ACTIVE SUPPRESSION OF VIBRATION MODES WITH PIEZOELECTRIC PATCHES: MODELING, SIMULATION AND EXPERIMENTATION

Asan Gani, MJE Salami – *SMIEEE,* Md. Raisuddin Khan
Department of Mechatronics Engineering,
International Islamic University Malaysia
Jalan Gombak, 53100, Kuala Lumpur
Malaysia
(asan@iiu.edu.my / momoh@iiu.edu.my / raisuddin@iiu.edu.my)

Abstract

Active vibration control of the first three modes of a vibrating cantilever beam using piezoelectric patches is examined in this paper. A model based on Euler-Bernoulli beam equation is adopted and extended to the case of three bonded piezoelectric patches which act as sensor, actuator and exciter respectively. The sensor and the actuator are collocated to achieve a minimum phase. A compensated inverse PID controller has been designed and developed to damp these modes. Simulation studies are carried using MATLAB. Individual controller has been designed for each mode and then combined in parallel to damp any of the three modes. Finally, the simulation results are compared and verified experimentally and the real-time implementation is carried out with xPC target toolbox in MATLAB.

Key Words

Piezoelectric materials, active vibration control, real-time implementation, Inverse-PID controller, xPC, MATLAB

1. Introduction

Advances in smart materials have shown an increased interesting application of smart material for structural mode damping. Some areas of applications are automobile, aerospace, and precision machining. Advancements in smart material technology have produced much smaller actuators and sensors with high structural integrity, making them suitable for use in many control applications. In contrast to passive damping which has fixed frequency range, piezoelectric materials can be used to damp a wider range of frequencies without adding much weight to the structure. Research in piezoelectric materials is continuously revealing different areas of application which when properly attached can improve the quality and products in manufacturing industries.

Active vibration control can be achieved using many techniques such as the modal approach for global structural dynamics control [1], [2] and wave suppression method [3]. Piezoelectric materials for active vibration control may be achieved either passively (with shunt circuit) [4]-[6] or actively. In shunt circuit techniques, the main role of piezoelectric material is to dissipate mechanical energy. This is achieved when mechanical work is done on an element and some portion of it is converted to and stored as dielectric energy. In a vibrating structure, a shunt network can be configured to accomplish vibration control by modifying the dynamics of the electrical system [7], [8]. A properly tuned shunt circuit can add significant damping to a structure. In active vibration suppression, an external power is applied to a piezoelectric material to produce force in opposite direction to that produced by vibrating structure at a particular position. The opposite forces cancel each other and thus help to reduce the vibration. Piezoelectric materials act as an actuator as well as a sensor in active vibration suppression of flexible structures.

A technique of damping the first three modes of a vibration beam using piezoelectric patches is discussed in this paper. This paper shows the reduction in piezoelectric sensor output under the effect of controller for the first three modes. A compensated inverse PID controller is designed to reduce multiple vibration modes of structures. The 'spillover' effect which is caused by the presence of uncontrolled or unmodeled modes within the bandwidth of the closed loop system is also considered in designing this controller. The controller developed for each mode is tested individually and later combined in parallel to control any of the three modes. The performance of the combined controller is discussed and a comparison is made between the individual and the combined controller.

2. Euler-Bernoulli Beam Model

In this section, the mathematical model for Euler beam as a continuous system with collocated piezoelectric sensor and actuator is developed. Various transfer functions for use in simulation studies are also discussed in detail.

2.1 Lateral Vibration of Beam

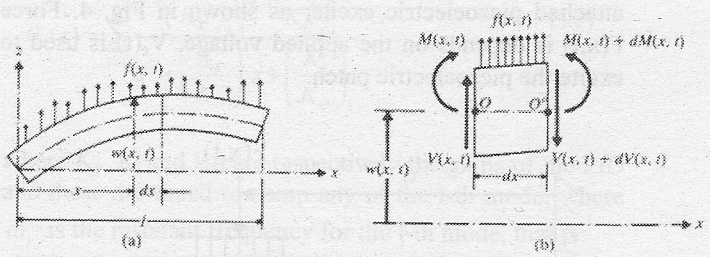

Fig. 1. Lateral vibration of beam [9]

Considering the equation of motion along the z-axis and the moment around y-axis at O leads to:

$$-(V+dV)+f(x,t)dx+V=\rho A(x)dx\frac{\partial^2 z(x,t)}{\partial t^2} \quad (1)$$

$$(M+dM)-M-(V+dV)dx+f(x,t)dx\frac{dx}{2}=0 \quad (2)$$

Inertia force acting on beam = $\rho A(x)dx\frac{\partial^2 z(x,t)}{\partial t^2}$ where ρ = mass density and $A(x)$ = cross sectional area.

Taking $dV=\frac{\partial V}{\partial x}dx$, $dM=\frac{\partial M}{\partial x}dx$ and $(dx)^2=0$, in equation (1),(2) gives:

$$-\frac{\partial^2 M}{\partial x^2}(x,t)+f(x,t)=\rho A(x)\frac{\partial^2 z(x,t)}{\partial t^2} \quad (3)$$

Based on Euler-Bernoulli or thin beam theory the relationship between bending moment and deflection is given by:

$$M(x,t)=EI(x)\frac{\partial^2 z}{\partial x^2}(x,t) \quad (4)$$

where E=Young's modulus and I(x) is the area moment of inertia of the beam cross section about the neutral axis. Substituting (4) in (3) yields:

$$EI(x)\frac{\partial^4 z}{\partial x^4}(x,t)+\rho A(x)\frac{\partial^2 z(x,t)}{\partial t^2}=f(x,t) \quad (5)$$

2.2 Model with Bonded Piezoelectric Patches

In Fig. 2 the dimension and the position of the attached piezoelectric patch on the beam is shown. A voltage $V_a(t)$ is applied to the piezoelectric patches.

Assuming the beam a one dimensional system, equation (5) can be further modified as:

$$EI(x)\frac{\partial^4 z}{\partial x^4}(x,t)+\rho A(x)\frac{\partial^2 z(x,t)}{\partial t^2}=\frac{\partial^2 M_a}{\partial x^2}(x,t) \quad (6)$$

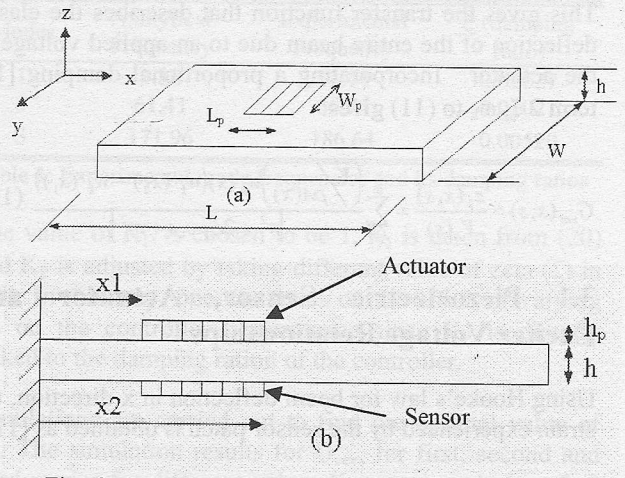

Fig. 2. Collocated piezoelectric patches on the beam

where M_a is the actuator induced bending moment. If the beam is bent by an external load into downward curvature the portion of the beam and piezo actuator above the neutral axis will experience tension. The moment M_a is then given by:

$$M_a=\bar{K}V_a(t) \quad (7)$$

$$\bar{K}=\frac{E_b I\kappa d_{31}}{h_a} \text{ and } \kappa=\frac{12E_a h_a[h+h_a]}{[2E_b h^3+E_a[(h+2h_a)^3-h^3]]}$$

To incorporate the placement of the piezo patch on the beam surface in x direction, Heaviside Step function is employed, so that the finite length of actuator can be accommodated in equation (7) and can be written as:

$$M=\bar{K}V_a(t)[H(x-x_1)-H(x-x_2)] \quad (8)$$

Using assumed mode approach, and substituting $z(x,t)=\sum_{k=1}^{\infty}w_k(x)q_k(t)$ and using (8) in (6) gives:

$$\frac{\partial^2 q_k(t)}{\partial t^2}+\omega_k^2 q_k(t)=\frac{\bar{K}V_a(t)}{\rho A(x)}(w_k'(x_2)-w_k'(x_1)) \quad (9)$$

3. Transfer Functions for Simulation Studies

Laplace transform of equation (9) gives:

$$q_k(s)[s^2+\omega_k^2]=\frac{\bar{K}(w_k'(x_2)-w_k'(x_1))}{\rho A(x)}V_a(s) \quad (10)$$

Since for the k-th mode, $z_k(x,s)=w_k(x)q_k(s)$ this equation then becomes:

$$z_k(x,s)=\frac{w_k(x)\bar{K}(w_k'(x_2)-w_k'(x_1))}{\rho A(x)[s^2+\omega_k^2]}V_a(s) \quad (11)$$

This gives the transfer function that describes the elastic deflection of the entire beam due to an applied voltage to the actuator. Incorporating a proportional damping [10] term $2\zeta_k\omega_k$ to (11) gives:

$$G_{vaz}(x,s)=\frac{z_k(x,s)}{V_a(s)}=\sum_{k=1}^{\infty}\frac{\left(\overline{K}/\rho A(x)\right)w_k(x)\left(w_k'(x_2)-w_k'(x_1)\right)}{\left[s^2+2\zeta_k\omega_k s+\omega_k^2\right]} \quad (12)$$

3.1 Piezoelectric Sensor, Actuator and Exciter Voltage Relationships

Using Hooke's law for beam deflection in x direction, the strain experienced by the sensor patch is obtained as [11]:

$$\varepsilon_b(x,t)=\frac{\partial u}{\partial x}=-\left(\frac{h}{2}+h_p\right)\frac{\partial^2 z(x,t)}{\partial x^2} \quad (13)$$

The strain introduced in the beam will produce an electric charge distribution per unit area in piezo sensor due to piezoelectric effect. The electric charge distribution is given by $q(x,t)=\frac{k_{31}^2}{g_{31}}\varepsilon_b$ where k_{31} is the electromechanical coupling constant and g_{31} is the piezoelectric stress constant. The total charge accumulated on the sensing layer can be found by integrating q(x,t) over the entire surface area of the piezo sensor and that is given by,

$$Q(t)=\int_{x1}^{x2}w_p q(x,t)dx=-w_p\left(\frac{h}{2}+h_a\right)\frac{k_{31}^2}{g_{31}}\frac{\partial z(x,t)}{\partial x}\Bigg|_{x1}^{x2} \quad (14)$$

Charged piezoelectric patches can be considered as a parallel plate capacitor, where the voltage across the layer is;

$$V_s(t)=\frac{Q(t)}{C_p(x2-x1)}=C_s\frac{\partial z(x,t)}{\partial x}\Bigg|_{x1}^{x2} \quad (15)$$

where C_p is the patch capacitance and x2-x1 is the length of piezo sensor and C_s is expressed as:

$$C_s=-w_a\left(\frac{h}{2}+h_a\right)\frac{k_{31}^2}{C_p g_{31}(x2-x1)}$$

Taking the Laplace transform of (15) gives

$$V_s(s)=\frac{C_s\overline{K}}{\rho A(x)}\sum_{k=1}^{\infty}\frac{\left(w_k'(x2)-w_k'(x1)\right)\left(w_k'(x2)-w_k'(x1)\right)}{\left[s^2+2\zeta_k\omega_k s+\omega_k^2\right]}V_a(s)$$

which can be written as

$$G_{vavs}(s)=\frac{V_s(s)}{V_a(s)}=\frac{C_s\overline{K}}{\rho A(x)}\sum_{k=1}^{\infty}\frac{\left(w_k'(x2)-w_k'(x1)\right)^2}{\left[s^2+2\zeta_k\omega_k s+\omega_k^2\right]} \quad (16)$$

Similarly relations for exciter voltage and sensor voltage can be derived using the geometry of the beam with attached piezoelectric exciter as shown in Fig. 4. Force F(x,t) is depends on the applied voltage, $V_e(t)$ is used to excite the piezoelectric patch.

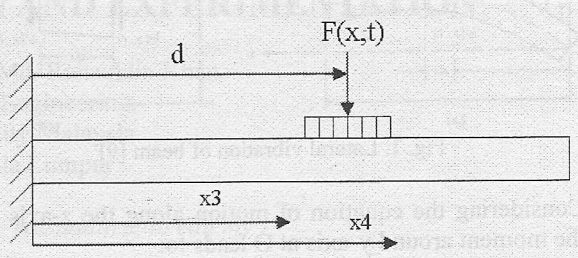

Fig. 4. Location of piezoelectric exciter on beam

The sensor voltage output for the applied exciter voltage derived from equations (10) – (16) is given below.

$$G_{vevs}(s)=\frac{V_s(s)}{V_e(s)}=C_s\sum_{k=1}^{\infty}\frac{\overline{K}\left[w_k'(x4)-w_k'(x3)\right]\left[w_k'(x2)-w_k'(x1)\right]}{\rho A(x)\left[s^2+2\zeta_k\omega_k+\omega_k^2\right]} \quad (17)$$

4. Controller Design

The structure of the closed loop system of the beam attached with piezoelectric sensor and actuators is shown in Fig 5.

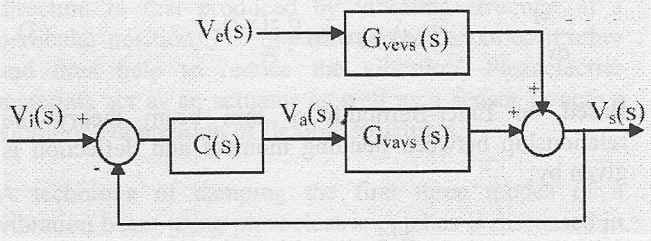

Fig. 5: Block diagram with feedback control for piezoelectric sensor output ($V_s(s)$)

Using the actuator voltage $V_a(s)$ as $V_a(s)=[V_i(s)-V_s(s)]C(s)$, the block diagram in Fig. 5 leads to the following closed loop transfer functions:

$$V_s(s)=\frac{G_{vevs}(s)V_e(s)}{1+C(s)G_{vavs}(s)}+\frac{C(s)G_{vavs}(s)V_i(s)}{1+C(s)G_{vavs}(s)} \quad (18)$$

It is desired to have $V_i(s)$ equal to zero as the role of the controller is only to eliminate the effects of the disturbance force F(x,t) which is controlled by its voltage $V_e(s)$.

The proposed controller in this paper is a 'compensated inverse PID' denoted as CIPID. The controller is developed by taking into consideration the effect of truncated modes which might cause the spillover effects [12],[13]. Hence the controller is designed to attenuate the first three modes so that

$$C_i(s) = \sum_{i=1}^{3} \frac{s\left(\frac{1}{K_D}\right)_i \left(s + \frac{K_P}{K_D}\right)_i}{s^2 + \left(\frac{K_P}{K_D}\right)_i s + \left(\frac{K_I}{K_D}\right)_i} \quad (19)$$

where K_P, K_I and K_D are respectively the gains of the PID and these are tuned to damp any of the i-th mode, where ω_i is the resonant frequency for the i-th mode, that is

$$\left(\frac{K_I}{K_D}\right)_i = \omega_i^2 \,, \left(\frac{K_P}{K_D}\right)_i = 2\zeta\omega_i \quad (20)$$

Using superposition rules, the CIPID controller can be extended to control the first three modes as shown in (19). The controller for each mode will be arranged in parallel. Fig. 6, shows the controller and beam with bonded piezoelectric. Basically the CIPID is used to damp the resonant peaks by placing poles at each resonant frequency. Changing K_P in the above equation will change the damping factor for each mode and this can control the resonant peak. However, higher damping factor doesn't imply that the peak will be always reduced; hence an optimal value of K_P is required for each mode. Simulation studies have been carried out with the transfer functions derived in section 3 so as to obtain optimal values of K_P for each mode. A digital lowpass filter is applied to the sensor output to remove any interference signal or noise.

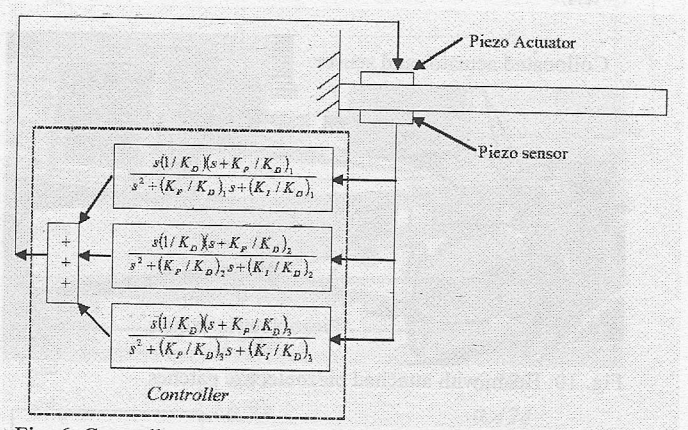

Fig. 6. Controller and beam bonded with piezoelectric patches

5. Simulation Results

The ability of the controller suggested in (19) to damp the resonant modes is studied in this section. Different values of K_P, K_I and K_D are taken to study their effects on the resonant modes. Simulation studies are carried out for the individual and combined controllers. In order to get more realistic simulation results, the damping values and mode frequencies used in the simulation studies are taken from the experimental results. The experimental and analytical damping ratios and mode frequencies are shown in Table I.

Modes	Analytical Frequency	Experimental Frequency	ζ (damping ratio)
1	9.80	11.14	0.02027
2	61.41	66.74	0.01021
3	171.96	186.64	0.00520

Table 1: Experimental mode frequencies and its damping ratios

The value of K_D is chosen to be 1, K_I is taken from (20) and K_P is adjusted by taking different value of zeta (ζ) in (20). In this way, one can focus on the effect of varying K_P on the controller performance since K_P is directly linked to the damping ration of the controller.

Simulations are carried out to find the optimal value of K_P. The simulation results for G_{vevs} for first, second and third modes for different values K_P are given in Fig. 7, 8 and 9 respectively. The resonant peak without controller is shown by "nocont" line. First mode peak is 18.6 dB, second mode is 17.7 dB and third mode is -11.5 dB. Table 2 shows the first mode reduction for resonant peak. Some smaller values of zeta cause undesirable shift to the resonant frequency and introduce new peaks close to the actual frequency. The reductions in peak for the second and third modes are given in Table 3. It is found that the lower damping values tend to increase the resonant peak, instead of reducing it and at the same time it introduces frequency shift. The optimum values are 11.141 for the first mode which gives 18.676dB peak reduction, 2.2228 for the second mode leading to 11.46dB of peak reduction and for the third mode is 11.141 with 2.9dB reduction in peak.

Zeta	K_P	First mode reduction (dB)
10	222.82	3.33
5	111.41	5.6
1	22.282	14.61
0.5	11.141	**18.676**
0.01	0.2228	14.05

Table 2: Reduction in first mode peak for different values of K_P

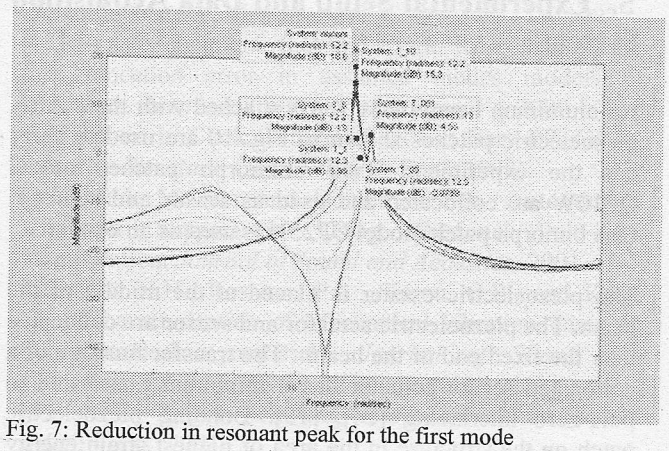

Fig. 7: Reduction in resonant peak for the first mode

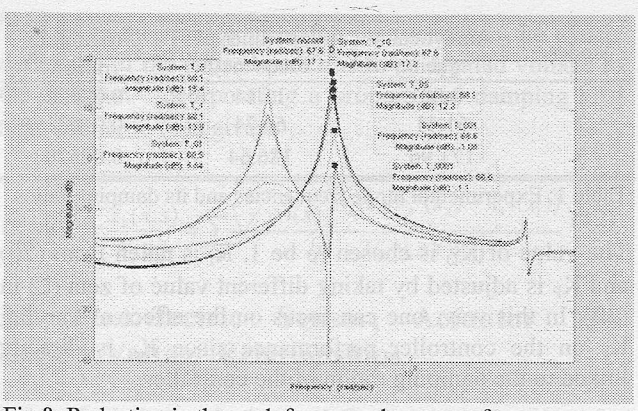

Fig 8: Reduction in the peak for second resonant frequency

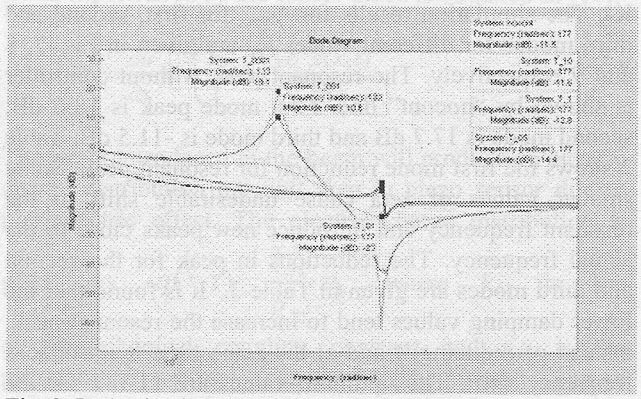

Fig. 9: Reduction in resonant peak for third mode

Zeta	K_P	Second mode reduction (dB)	Third mode reduction (dB)
10	222.82	0.4	0.1
1	22.282	3.4	1.3
0.5	11.141	5	**2.9**
0.1	2.2282	**11.46**	11.5
0.01	0.2228	18.38	-22.1
0.001	0.02282	18.4	-30.6

Table 3: Reduction in second and third mode peaks for different values of K_P

5. Experimental Setup and Data Acquisition System

An aluminum beam (6061 T651) attached with three ACX piezoelectric patches shown in Fig. 10 are used to carry out the experiment. Two unimorph patches model QP10W are collocated and used as sensor and actuator. One bimorph patch model QP25N is used as an exciter.

The piezoelectric exciter is placed at the middle of the beam. The piezoelectric actuator and sensor are collocated near the fixed end of the beam. The transfer function of a collocated sensor-actuator has a minimum phase due to pole-zero interlacing [14], [15]. Bonding piezoelectric patch on the structure in the area of highest strain energy will add most damping. It has been reported in [6], [17] that the highest strain energy for the first three modes is at clamped boundary of the cantilever beam. As reported in [17] an analytical equation can be used to accurately predict the optimum position of piezoelectric patches. Based on this, the piezoelectric sensor and actuator are attached at about 15 mm away from the clamped end of the beam

Two linear power amplifiers are used in this setup. Both amplifiers have a gain of up to 20 and output voltage of ±200V. A Keyence laser displacement sensor model LK-081 is used to measure the beam tip displacement. National instruments (NI) data acquisition card model PCI-MIO-16XE-10 is used to acquire analog signal from the piezoelectric sensor. Control signal is sent to piezoelectric actuator through output channel of the card. A four channel HP-Dynamic signal analyzer (DSA) model HP-35670A, is used to obtain beam resonant frequencies and respective damping ratios. Controlled and uncontrolled responses of the beam are measured and analyzed using the DSA. Real-time implementation is carried out using xPC Target toolbox in MATLAB. It is a high-performance, host-target prototyping environment that enables the connection or Simulink models to physical systems and execute them in real-time on PC-compatible hardware [18]. The schematic diagram for the experimental setup is shown in Fig. 11. HP-DSA is used to obtain transfer functions under controlled and uncontrolled condition. Ch3/Ch1 will measure transfer function for piezo-sensor output to input excitation signal (G_{vevs}).

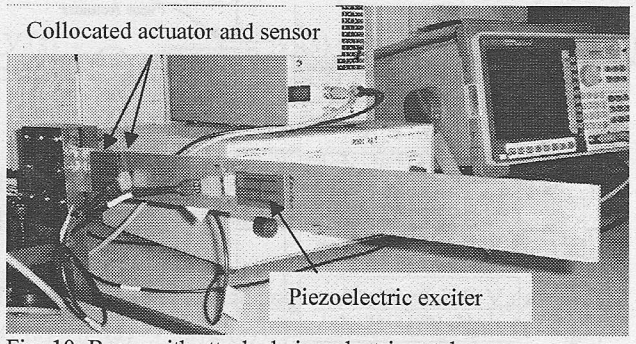

Fig. 10: Beam with attached piezoelectric patches

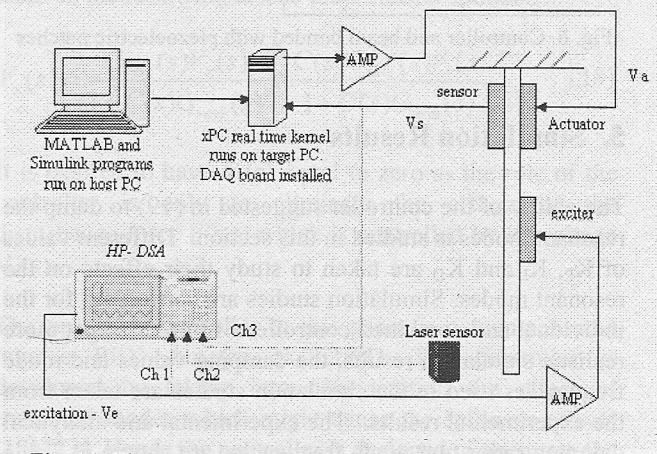

Fig. 11. The experimental setup for active vibration control

6. Experimental Results

The beam is excited at its resonant frequencies as given in Table 1. Experimental results for reduction in G_{vevs} for individual controller are summarized in Table 4.

	First Mode	Second mode	Third mode
Uncontrolled	1.2496	2.4594	0.02583
Controlled	0.1765	0.8817	0.02374
Reduction	1.0731	1.5777	0.00209
Reduction (dB)	**17.00**	**8.910**	**0.73287**
Reduction (%)	**92.05**	**64.15**	**8.10**

Table 4 : Performance of the third mode controller: G_{vevs} *(V/V)*

Performance of the combined controller is tested by exciting the beam with sweep sine signal of frequency range 3 to 203 Hz, which comprises the first three resonant mode frequencies. The reductions of resonant peaks in dB under effects of combined controller are shown in Fig. 12 and compared with the individual in Table 5.

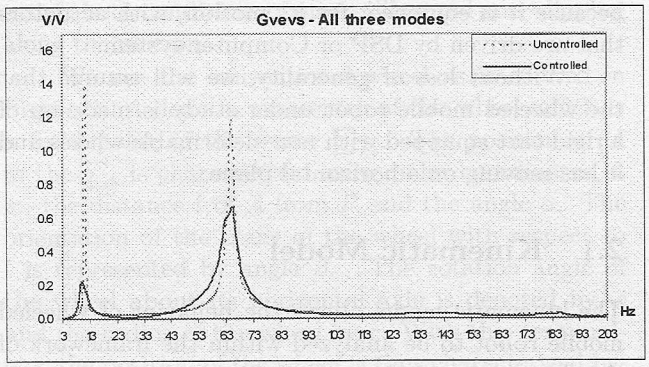

Fig. 12: Controlled and uncontrolled gain for G_{vevs} for first three modes

	Individual controller	*Combined controller*
1st	***17.00***	***17.07***
2nd	***8.91***	***6.827***
3rd	***0.73***	***0.424***

Table 5: Reduction in resonant peaks in dB

7. Conclusion

The design, implementation and testing of an inverse type PID controller for active vibration suppression of a beam are presented in this paper. The results of the real-time implementation of the controller using xPC target are found to be very close to that of simulation studies which actually demonstrates the effectiveness of this technique. In general for G_{vevs}, the individual controller has shown better performance over the combined controller for second and third modes while the results are almost similar for the first mode. The drop in resonant peaks for the combined controller is believed to be caused by the coupling effects.

References

[1] L. Meirovitch and J.K Bennighof, Modal Control of traveling waves in flexible structures, *Journal of Sound Vibration, 111*, 1986, 131-144.

[2] D. R. Morgan, An adaptive modal based active control system, *Journal of acoustical society of America, 89(1),* 1991, 248-256.

[3] B. R. Mace, Active control of flexural vibrations, *Journal of Sound and Vibration, 114 (2)*, 1987, 253-270.

[4] Hagood, N.W., and von Flotow, A.H., Damping of Structural Vibrations with piezoelectric Materials and Passive Electrical Network, *Journal of Sound and Vibration, 146(2),* 1991

[5] S Y Wu, Method for multiple mode shunt damping of structural vibration using single PZT transducer, *Proceedings SPIE, Smart Structures and Intelligent System,* March 1998

[6] John J. Granier, Jason Hundhausen, and Gabriel E. Gaytan, Passive Modal Damping with Piezoelectric Shunts, *Los Alamos National Labs,* 2001

[7] Giovanni Caruso, A critical analysis of electric shunt circuits employed in piezoelectric passive vibration damping, *Smart materials and structures*, 2001

[8] H. R Pota, S O Reza Moheimani and Matthew Smith, Resonant controller for smart structures, *Smart Materials and Structures*, 2002

[9] Singiresu S. Rao, *Mechanical Vibrations* (Addison Wesley, 1995)

[10] S. O. Reza Moheimani, Experimental Verification of the Corrected Transfer Function of A Piezoelectric Laminate Beam, *IEEE Transactions on Control Systems Technology, Vol. 8*, 2000.

[11] C. R. Fuller, S. J. Elliott & P.A. Nelson, *Active Control of Vibration* (Academic Press, 1996).

[12] R. L. Clark, "Accounting for out-of-bandwidth modes in the assumed modes approach: Implications on collocated output feedback control," Trans. ASME J. Dynamic System., Measurement, Contr., vol. 119, 1997

[13] Reza Moheimani, S.O and Clark, R.L., Minimizing the truncation error in assumed modes models of structures, *American Control Conference, V4*, 2000

[14] Robert L. Clark, William R. S and Gary PP. Gibbs, *Adaptive Structure,* (John Wiley & Sons, 1998).

[15] Mark McEver and Donald J. Leo, Autonomous Vibration Suppression Using On-Line Pole-Zero identification, *Journal of Sound and Acoustics,* 2001

[16] Law H.H., Rossiter, P.L., Simon, G.P., and Koss, L.L., Characterization of Mechanical vibration damping by piezoelectric materials, *Journal of Sound and Vibration, Vol. 197*, 1996

[17] xPC Target Selecting Hardware Guide-Manual *(MathWorks, 2001)*